Title:
A Comparative Study between NURBS Surfaces and Voxels to Simulate the Wear Phenomenon in Micro-EDM

Authors:
Anthony Surleraux, surlerauxAB@cardiff.ac.uk, Cardiff University, UK
Jean-Philippe Pernot, jean-philippe.pernot@ensam.eu, Arts et Métiers ParisTech, France
Samuel Bigot, bigotS@cardiff.ac.uk, Cardiff University, UK

Keywords:
Shape modeling and optimization, Continuous vs. discrete representations, Surface warping, Haussdorf metric

DOI: 10.14733/cadconfP.2015.236-240

Introduction:

Micro Electrical Discharge Machining (micro-EDM) is a micro-manufacturing process that involves the removal of material through electrical discharges. Its main strength resides in the fact that it is able to machine any electrically conductive material independently of its hardness [2]. The process involves two electrodes (one being referred to as the tool while the other is the workpiece) that are submitted to an electrical current and immerged in a dielectric fluid. As the distance separating both electrodes decreases, there is a point (known as the machining gap) where the dielectric fluid isn't able to insulate both electrodes from each other anymore and breaks down leading to the apparition of a plasma channel between both electrodes. The resulting thermal energy leads to melting and vaporization of the material on both electrodes and the removal of material as craters.

The main issue is that material is also removed from the tool (tool wear) and therefore influences the final shape obtained on the workpiece. The influence of tool wear is significantly greater when tackling with micro-scale features. Most previous efforts have been focused on the modelling of single-spark discharges through the solving of thermal equations and specific boundary conditions. A recent work has tackled with the geometrical simulation of a whole process through the use of Z-maps but those are inherently limited when it comes to representing overhangs.

In this paper, two new simulation techniques are introduced and compared with respect to experimental results. The first approach uses NURBS as models for the tool and workpiece while the second uses voxels embedded in an octree data structure. The Haussdorf metric is used to compare the simulation results with the experimental ones.

Main Idea:

Overview

The main idea is to develop a geometrical simulation method with the final objective of optimizing the initial shape of the tool by adding material on it to counteract the effects of tool wear. In order to do so, the simulation must be fast considering that the optimization method is likely to require a great deal of iterations. Actually, in a later stage, this method will take part to a shape optimization process where tens of simulations will be performed (Fig. 1).

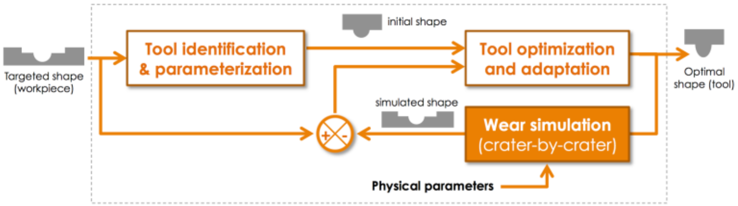

Fig. 1: The crater-by-crater simulation module plugged within a shape optimization loop.

Two methods using different geometric representations and associated algorithms have been developed and tested against experimental results. The first approach uses NURBS as models for the tool and workpiece while the second uses voxels embedded in an octree data structure. In both cases, the simulation loop is the same [1]:

1. For the current depth, the minimum distance d_{min} between both electrodes is found;
2. If d_{min} is bigger than the machining gap M_g, the tool is brought closer to the workpiece and the process goes back to 1 with a new depth;
3. If d_{min} is smaller than M_g, it is considered that a spark can appear and the geometries are modified to account for craters. The process than goes back to 1 except if the simulation has reached its objective depth in which case the simulation ends.

The NURBS method

In the NURBS method, both electrodes are modelled as single NURBS patches. The patches are then refined using the Boehm's knot insertion algorithm [4]) in order to obtain a million (1000x1000) control points for each patch. In this case, the surfaces are continuous representations what makes possible the computation of mathematical magnitudes such as the derivatives. The crater insertion method is illustrated by Fig. 2 and implements the surface warping technique.

For the current depth, the minimum distance search is done with the use of Particle Swarm Optimization (PSO) with four variables that are the NURBS patches parameters [3]. The output gives two points $S_t(u_t,v_t)$ and $S_w(u_w,v_w)$.

Then, it is supposed that, during the manufacturing process, all sparks transfer the same energy therefore removing the same volumes V_t and V_w for each iteration. Those volumes are computed by modelling the craters as spherical caps and experimentally measuring the mean depth Dc_t, Dc_w and radius Rc_t, Rc_w of craters. This enables the definition of the spherical cap's support sphere.

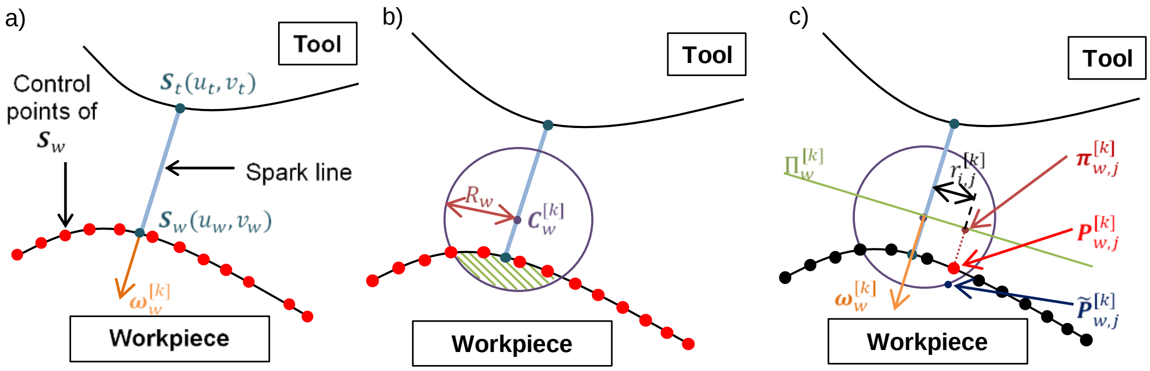

Fig. 2: Definition of the various elements involved in the crater insertion process.

The case considered here is the insertion of a crater on the workpiece (subscript w). As shown in Fig. 2(a), a warping unit vector is computed as in Eq. 1.1.

$$\boldsymbol{\omega}_{\boldsymbol{w}} = -\frac{\boldsymbol{S}_t(u_t,v_t)-\boldsymbol{S}_w(u_w,v_w)}{\|\boldsymbol{S}_t(u_t,v_t)-\boldsymbol{S}_w(u_w,v_w)\|} \tag{1.1}$$

The support sphere position has to be determined in the next step. Its center lies on the spark line as shown in Fig. 2(b). The exact position of the sphere's center is calculated with the condition that a volume V_w has to be removed (hashed section of Fig. 2(b)). That position is calculated using an iterative dichotomy method.

The final step is to move the control points that are inside the sphere to its boundary as illustrated in Fig. 2(c). Here, the control points are moved in the direction $\boldsymbol{\omega}_w^{[k]}$ so as to reach the boundary of the previously identified sphere. Due to the great number of control points, the approximation is possible.

The voxels method

The voxels in this method are embedded in an octree structure and used to model both electrodes in a volumetric and discrete manner. The octree provides with the ability to represent large sections of the volumes as bigger voxels and therefore reduces memory usage. Additionally, it provides with a hierarchical structure that is useful when querying a specific voxel. An octree is composed of nodes that have a parent node and up to eight children nodes. A node with no children is said to be a leaf node. The topmost node in the structure is called the root node.

For the current depth of the simulation process, the minimum distance search is an iterative process that uses couples of nodes. For each couple, the process involves finding the lower and upper bounds of the minimum distance between them. If both nodes are leaves the minimum distance is the lower bound. Additionally, if one of the nodes is a leaf and the other isn't, the minimum distance can be bounded more precisely.

The minimum distance algorithm starts with the couple of the root nodes of each octree and, for each possible couple of their children, the minimum distance is bounded. The couples are then culled and only those with a lower bound smaller than the supremum (least upper bound) are kept for the next iterations. The process is then repeated with the children of the remaining couples until a fixed number of iterations is achieved. An early exit condition is possible in the case where a couple of leaves nodes have a minimum distance smaller than the machining gap M_g. Another exit condition is provided in the case where a couple has an upper bound smaller than M_g. If the resulting couples aren't made of leaves, the algorithm is re-applied on it.

Once the closest nodes have been identified, the crater insertion method on an octree starts with the root node. The children are tested for intersection with a sphere defined in the same way as in section 1.2. Children completely inside the sphere are deleted while children intersecting the boundary of the sphere are kept for the next iteration. The process stops after a fixed number of iterations.

Experimental validation and comparative study

In order to assess the performances of each method, an experiment was devised in order to measure the shape differences between simulated and experimental results. The tool that was used is of a spherical shape as visible in Fig. 3. and it has been obtained through wire-dressing of a cylindrical electrode of nominal diameter 300µm. The nominal diameter of the sphere is 250µm. This tool was measured with the help of a micro-tomographer of a resolution of 1µm. The result was exported as a three-dimensional mesh (Fig. 3). The tool was also measured in the same manner after the experiment.

The NURBS elements used were a sphere of diameter 250µm for the tool and a flat square surface with a side length of 500µm for the workpiece as shown in Fig. 4(a). The voxel tool was created from the micro-tomographer STL files as shown in Fig. 4(b). The workpiece is a cube of dimension 512 µm.

Proceedings of CAD'15, London, UK, June 22-25, 2015, 236-240

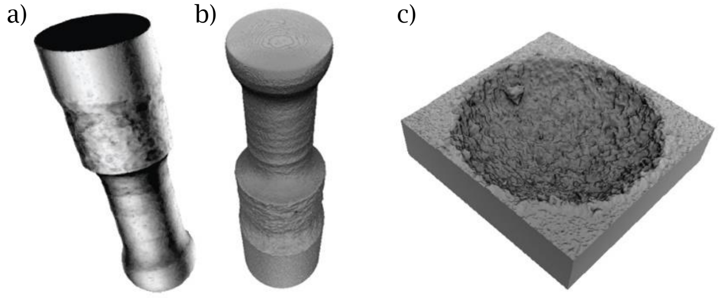

Fig. 3: 3-D mesh of the experimental tool: a) before and b) after machining, c) workpiece after machining.

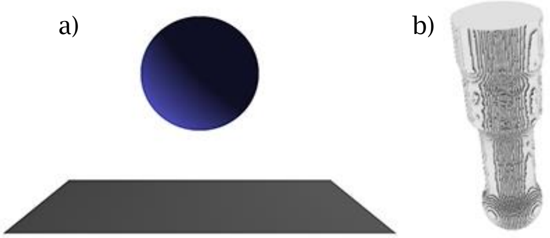

Fig. 4: a) NURBS models of the sphere-like tool and the workpiece b) Voxel model of the tool.

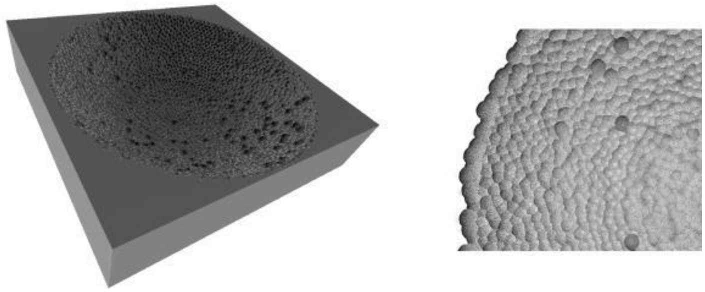

Fig. 5: Voxel workpiece after simulation (left) and details of the craters (right)

Those two models do represent the same extremity of the tool using a sphere-like shape. The NURBS simulation ended after 2040 minutes while the voxels simulation took 126 minutes and is therefore more than 16 times faster. After the simulation, the resulting models (NURBS and voxels, voxels are shown Fig. 5) were compared to the experimental ones with the use of the Hausdorff metric defined in Eq. 1.2. where X and Y are two sets of points.

$$d_H(X,Y) = \max\{\underbrace{sup}_{x\in X}\underbrace{inf}_{y\in Y} d(x,y), \underbrace{sup}_{y\in Y}\underbrace{inf}_{x\in X} d(x,y)\} \tag{1.2}$$

The Hausdorff metric results are tabulated in Tab. 1 and are visible in Fig. 5. Tab. 1 gives the minimum, maximum, mean and RMS values of each set of sampled points' Hausdorff distance.

	NURBS		Voxels	
	Tool	Workpiece	Tool	Workpiece
d_H min (µm)	0.000000	0.000107	0.008184	0.000000
d_H max (µm)	8.629291	14.886533	2.163380	14.917241
d_H mean (µm)	1.449477	3.073571	0.858142	0.718315
d_H RMS (µm)	2.521132	3.626015	0.971600	1.682061

Tab. 1: Hausdorff metric results.

Fig. 6 depicts the maps of the calculated Hausdorff distances. A red color represents a small difference between the experimental and simulated elements while a blue color indicates a larger difference.

Conclusions:

Considering the Hausdorff distance RMS values, both methods offer a good prediction of the experimental results with values in the range of 2-3 µm for the NURBS method and 1-2 µm for the voxel method. Those values are to be compared with the dimensions of the models (bounding box diagonal of 403 µm for the workpiece and 366 µm for the tool). While the NURBS method offers geometries with no sharp edges, the voxel method is significantly faster and therefore more efficient when used as part of a shape optimization loop.

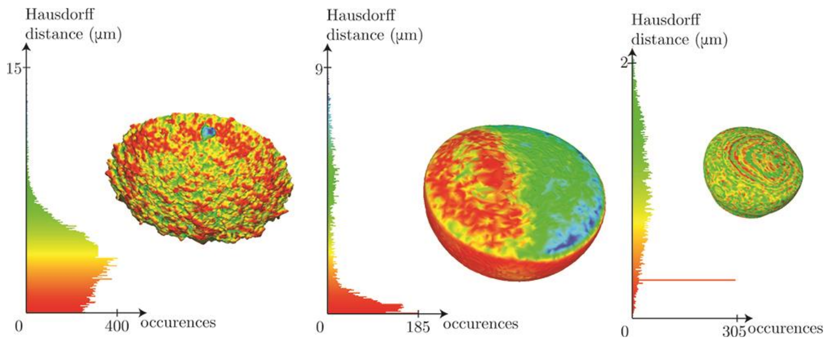

Fig. 6: Hausdorff distance maps.

Acknowledgements:

This work was supported by the Engineering and Physical Sciences Research Council [EP/F056745/1, EP/J004901/1].

References:

[1] Bigot, S.; Pernot, J.-P., Surleraux, A., Elkaseer, A.: Micro-EDM numerical simulation and experimental validation, Proceedings of the 10th International Conference on Multi-Material Micro Manufacture, 2013. http://dx.doi.org/10.3850/978-981-07-7247-5_414.

[2] Ho, K. H.; Newman, S. T.: State of the art electrical discharge machining (EDM International Journal of Machine Tools and Manufacture, 43, 2003, 1287-1300, http://dx.doi.org/10.1016/S0890-6955(03)00162-7.

[3] Kennedy, J., Eberhart, R.: Particle Swarm Optimization, Proceedings of IEEE International Conference on Neural Networks IV, 1995, 1942–1948, http://dx.doi.org/10.1109/ICNN.1995.488968.

[4] Piegl, L.; Tiller, W.: The NURBS Book, Springer, 1997, http://dx.doi.org/10.1007/978-3-642-59223-2.